

AD-A044 280

EIKONIX CORP BURLINGTON MA

DESIGN AND FEASIBILITY STUDY OF HOC AS A VAN MOUNTED STEREO MOD--ETC(U)

F/G 20/6

JUL 77

DAAK70-77-C-0027

UNCLASSIFIED

EC/2106601-FR

ETL-0109

NL

| OF |

AD  
A044280



END  
DATE  
FILMED  
10-77  
DDC

ADA 044280

EIKONIX

1  
NW



DDC  
SEP 19 1977  
RECEIVED

FILE COPY

DISTRIBUTION STATEMENT A  
Approved for public release;  
Distribution Unlimited

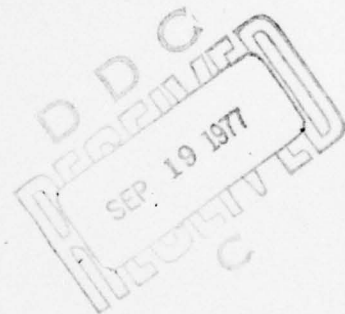
**EIKONIX** corporation  
103 terrace hall avenue  
burlington, mass. 01803  
tel. (617) 273-0350

ETL-0109

**DESIGN AND FEASIBILITY STUDY  
OF HOC AS A VAN MOUNTED STEREO  
MODEL DIGITIZER**

Prepared for U. S. Army Engineer Topographic Laboratories

Approved for public release, distribution unlimited.



DISTRIBUTION STATEMENT A  
Approved for public release;  
Distribution Unlimited

Unclassified

SECURITY CLASSIFICATION OF THIS PAGE (When Data Entered)

REPORT DOCUMENTATION PAGE		READ INSTRUCTIONS BEFORE COMPLETING FORM	
1. REPORT NUMBER ETL 0109	2. GOVT ACCESSION NO.	3. RECIPIENT'S CATALOG NUMBER	
4. TITLE (and Subtitle) Design and Feasibility Study of HOC as a Van Mounted Stereo Model Digitizer,		5. TYPE OF REPORT & PERIOD COVERED Contract Report Final Report	
7. AUTHOR(s)		6. PERFORMING ORG. REPORT NUMBER EC/2106601-FR	
9. PERFORMING ORGANIZATION NAME AND ADDRESS EIKONIX Corporation 103 Terrace Hall Avenue Burlington, Ma. 01803		8. CONTRACT OR GRANT NUMBER(s) DAAK-70-77-C-0027 / new	
11. CONTROLLING OFFICE NAME AND ADDRESS U. S. Army Engineer Topographic Laboratories Fort Belvoir, Virginia 22060		10. PROGRAM ELEMENT, PROJECT, TASK AREA & WORK UNIT NUMBERS 12 66 p.	
14. MONITORING AGENCY NAME & ADDRESS (if different from Controlling Office)		12. REPORT DATE 12 Jul 1977	
		13. NUMBER OF PAGES 64 (sixty-four)	
		15. SECURITY CLASS. (of this report) Unclassified	
		15a. DECLASSIFICATION/DOWNGRADING SCHEDULE	
16. DISTRIBUTION STATEMENT (of this Report) Approved for public release; distribution unlimited.			
17. DISTRIBUTION STATEMENT (of the abstract entered in Block 20, if different from Report)			
18. SUPPLEMENTARY NOTES			
19. KEY WORDS (Continue on reverse side if necessary and identify by block number) (Heterodyne optical correlation) Automated Stereo Compilation, Stereomodel digitizer.			
20. ABSTRACT (Continue on reverse side if necessary and identify by block number) This report documents the results of the evaluation of the feasibility and applicability of a potential HOC system as a van mounted stereomodel digitizer. A HOC system model has been developed and it is evaluated by considering the tolerance specifications of the optical, mechanical and electronic subsystems as a function of their required performance characteristics. The results of this study indicate that a potential HOC system is highly competitive in its application as a van mounted stereomodel digitizer. Finally a conceptual design for a prototype HOC system has been presented and its potential advantages			

D D C  
SEP 19 1977  
RESISTED  
C

→ next page

Unclassified

SECURITY CLASSIFICATION OF THIS PAGE(When Data Entered)

Block 20

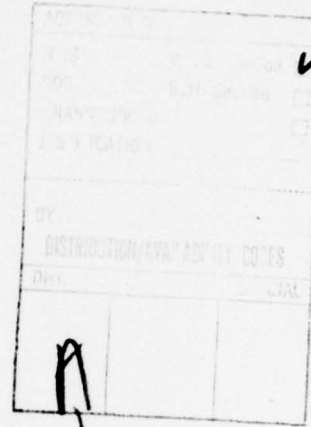
over other automated compilation systems <sup>were</sup> have been outlined.

Unclassified

SECURITY CLASSIFICATION OF THIS PAGE(When Data Entered)

## TABLE OF CONTENTS

<u>Section</u>	<u>Title</u>	<u>Page</u>
1	INTRODUCTION	1
2	BASIC HOC SYSTEM CONCEPTS	3
2.1	Introduction	3
2.2	Principle of Operation	3
2.3	Experimental HOC System	11
2.4	Stereo Compilation Procedure	15
2.5	Summary	20
3	PROPOSED PROTOTYPE SYSTEM MODEL	22
3.1	Introduction	22
3.2	System Requirements	22
3.3	System Model Options	23
4	HOC SYSTEM EVALUATION	30
4.1	Introduction	30
4.2	Effects of Vibration on Correlation Coefficient Measurements	30
4.3	Effects of Mechanical and Thermal Drift on Normalized Correlation Coefficient Measurement	34
4.4	Tolerance Requirements of Translation Stages and their Effect on Measurement Accuracy	37
4.5	Evaluation of Array Detector Sensitivity and Laser Power Requirements	37
4.6	Evaluation of the Effect of Input Transparency Format Geometry on the Performance of the HOC System	41
4.7	Summary	47
5	PROPOSED PROTOTYPE HOC SYSTEM DESIGN	48
5.1	Introduction	48
5.2	System Description	48
5.3	Data Processing Requirements	55
5.4	Unique Characterization of the Proposed HOC System	57
6	CONCLUSIONS	59
6.1	Introduction	59
6.2	Recommendations	60
7	REFERENCES	62



## 1 INTRODUCTION

During the last several years considerable progress has been made with regard to the demonstration of the basic concepts of heterodyne optical correlation as well as the potential application to stereo compilation. Earlier, under various investigations supported by the Center for Coherent Optics, USAETL, an experimental bread board system based on the HOC concept has been designed, fabricated and evaluated. The present study, of which this document is the final report, deals with the evaluation of the feasibility and applicability of a potential HOC system under adverse environmental factors demanded by field applications. The main purpose of this investigation is to study the design and feasibility of HOC as a van mounted stereo-model digitizer.

The specific objectives of this effort are:

- (a) To develop a HOC system model that is representative of a potential operating instrument and evaluate the complexity of the system to meet the required performance characteristics.
- (b) To evaluate the characteristics and tolerances of the optical, mechanical and electronic subsystems from the point of view of fabrication, maintenance and other operational requirements such as vibration and thermal isolation.
- (c) To conceptually design a follow-on prototype HOC system incorporating the results of the above study and specify the potential system characteristics.

This report is organized into six chapters. For the purpose of providing continuity to this report, the principle of operation of the concept of heterodyne optical correlation is presented in the second chapter. The experimental HOC system is also described and its operating procedure outlined. In the

third chapter the various system model options are considered and the arguments relating to the selection of a specific system model are included. In the fourth chapter the HOC system is evaluated by considering the tolerance specifications of the optical, mechanical and electronic subsystems as a function of their required performance characteristics. A conceptual design of a prototype HOC system is presented in the fifth chapter along with its potential advantages over other automated compilation systems. Finally the conclusions and recommendations based on this investigation are summarized in the sixth chapter.

## 2 BASIC HOC SYSTEM CONCEPTS

### 2.1 Introduction

All automated stereo-compilation instruments are based on the ability to match conjugate images and automatically determine the parallax difference. Conjugate images are matched using image correlation. The HOC System is an optical correlation system that performs the two-dimensional correlation of the conjugate images on a superimposed image plane. Considerable literature already exists on the various aspects and the unique characteristics of the HOC concept (1). However, for the purpose of continuity in this report, a brief introduction to the concept of heterodyne optical correlation is presented and the basic stereo compilation mensuration procedure is outlined. The operating procedure is described within the context of the experimental HOC system at the Center for Coherent Optics, USAETL, since, in general the procedure is highly dependent on the system design.

### 2.2 Principle of Operation

The basic optical arrangement of the HOC system consists of two projectors each of which projects an image of the transparency onto a common image plane using coherent light. The basic configuration of the system is illustrated in Figure 2-1. In this arrangement transparencies 1 and 2 form the stereopair. Let  $t_1(x_1, y_1)$  be the amplitude transmittance of transparency 1. The coordinate system  $(x_1, y_1)$  refers to the photocoordinates of transparency 1. Similarly the amplitude transmittance of transparency 2 is  $t_2(x_2, y_2)$ . The coordinate system  $(x_2, y_2)$  refers to the photocoordinates of transparency 2. In the final common image plane, the superimposed amplitude distribution is given by

$$i(x, y) = t_1 \left[ \frac{x}{k_1}, \frac{y}{k_1} \right] + t_2 \left[ \frac{x}{k_2} + x_0, \frac{y}{k_2} + y_0 \right] \quad (2.1)$$

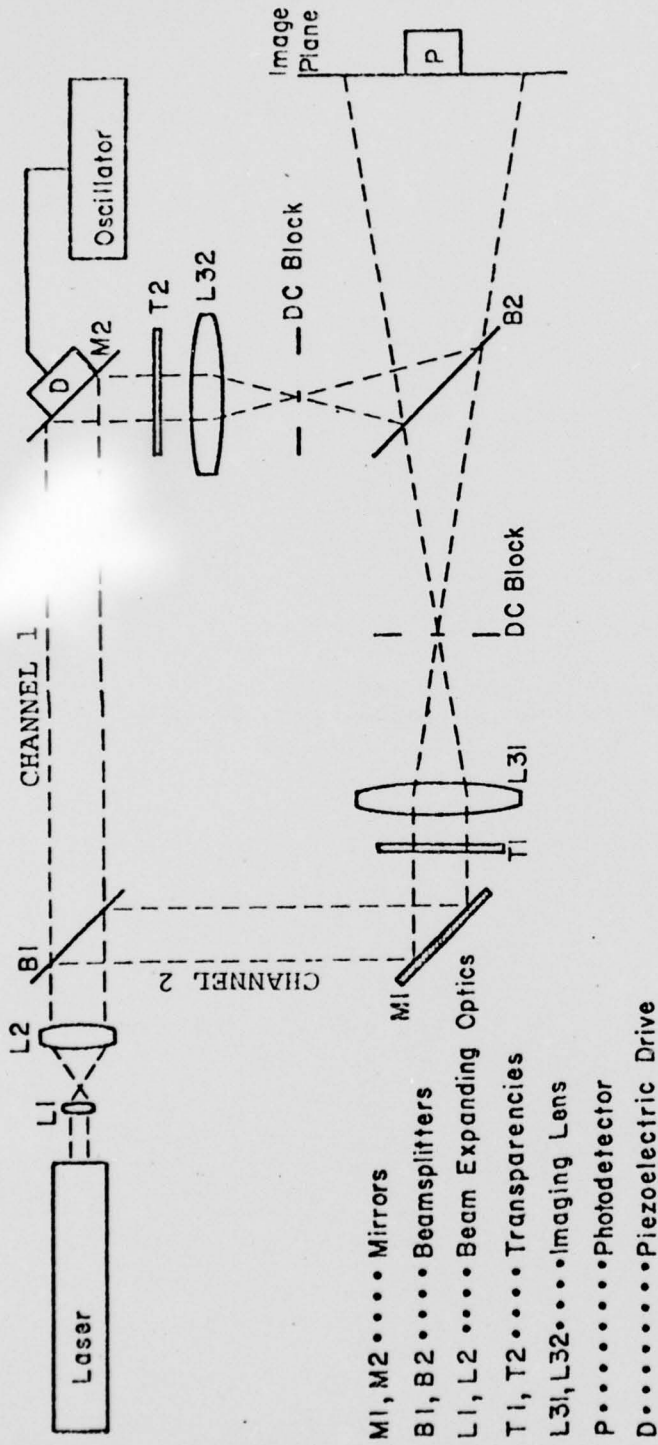


FIGURE 2.1 BASIC HETERODYNE OPTICAL CORRELATION SYSTEM

where

$$k_1 x_1 = x, k_1 y_1 = y \quad (2.2)$$

$$k_2 (x_2 - x_0) = x, k_2 (y_2 - y_0) = y.$$

$k_1$  and  $k_2$  are magnification factors associated with projectors 1 and 2. In a very general case  $k_1$  and  $k_2$  can also be made dependent on  $(x, y)$  (as in the case of rectifiers or anamorphic magnifiers) but for the purposes of this treatment  $k_1$  and  $k_2$  are assumed to be constant and equal to unity. Hence equation (2.2) becomes

$$i(x, y) = t_1(x, y) + t_2(x+x_0, y+y_0) \quad (2.3)$$

The photodetector senses the intensity rather than the amplitude. The intensity distribution is given by the square of equation (2.3) as

$$I(x, y) = \left| t_1(x, y) \right|^2 + \left| t_2(x+x_0, y+y_0) \right|^2 + 2t_1(x, y)t_2(x+x_0, y+y_0)\cos \frac{2\pi}{\lambda} \Delta(x, y) \quad (2.4)$$

where  $\lambda$  is the wavelength of the light and  $\Delta(x, y)$  is the optical path difference between two beams. The third term in the above expression is an interaction term resulting from the fact that the laser light illuminating the transparencies are coherent. One of the major objectives of the measurement procedure is to

detect the amplitude of the cosine modulation represented by the third term in the above expression. This amplitude can be measured by modulating the optical path difference (OPD)  $\Delta(x, y)$ . The OPD  $\Delta(x, y)$  can be modulated in many ways and more detailed discussion is presented later in this report on the significance of this measurement on the overall system performance. In general, the measurement of the peak to peak value of the intensity function defined by equation (2.4) permits independent determination of the amplitude of the cosine modulation. When the OPD has a linear time modulation, the intensity distribution given by equation (2.4) becomes

$$I(x, y, t) = \left| t_1(x, y) \right|^2 + \left| t_2(x+x_0, y+y_0) \right|^2 + 2t_1(x, y)t_2(x+x_0, y+y_0)\cos \frac{2\pi}{\lambda}(\Delta_0(x, y)+Vt) \quad (2.5)$$

where  $V/\lambda$  is the frequency of modulation.

The detector in the final image plane, has an aperture of area  $A$  and its output signal at point  $P$  in the image plane is given by the integral

$$S(P, t) = K \iint_A I(x, y, t) dA \quad (2.6)$$

where  $K$  is a constant of proportionality dependent on the photodetector response

$$S(P, t) = K \left[ \iint_A \left| t_1(x, y) \right|^2 dA + \iint_A \left| t_2(x+x_0, y+y_0) \right|^2 dA + 2 \iint_A t_1(x, y)t_2(x+x_0, y+y_0)\cos \frac{2\pi}{\lambda} (\Delta_0(x, y)+Vt) dA \right] \quad (2.7)$$

The first two terms of the above equation are d. c. signals while the third represents an a. c. signal at the beat frequency  $(V/\lambda)$ .

When the optical path difference  $\Delta_o(x, y)$  is essentially constant over the aperture area  $A$ , the a. c. part of the detector signal can be written as

$$S_V(P, t) = 2K \cos \frac{2\pi}{\lambda} (\Delta_o + Vt) \iint t_1(x, y) t_2(x+x_o, y+y_o) dA \quad (2.8)$$

Hence the a. c. part is a signal at frequency  $V/\lambda$  having a phase of  $\Delta_o$  and an amplitude

$$S_V(P) = 2K \iint t_1(x, y) t_2(x+x_o, y+y_o) dA \quad (2.9)$$

The above expression represents the correlation between the two amplitude transmittances for the displacement  $(x_o, y_o)$ . Two additional measurements are necessary to normalize the above correlation function. When only transparency 1 is illuminated, the d. c. output is given by

$$S_{01} = K \iint |t_1(x, y)|^2 dA. \quad (2.10)$$

Similarly, when transparency 2 is illuminated

$$S_{02} = K \iint |t_2(x, y)|^2 dA \quad (2.11)$$

with these three measurement values the normalized correlation coefficient

can be computed for a given  $(x_o, y_o)$  separation between transparencies from

$$C_{12}(x_o, y_o; P) = \frac{\int_A t_1(x, y) t_2(x+x_o, y+y_o) dA}{\left[ \iint t_1(x, y)^2 dA \iint |t_2(x+x_o, y+y_o)|^2 dA \right]^{1/2}}$$

$$= \frac{S_V(P)}{2 [S_{01} S_{02}]^{1/2}} \quad (2.12)$$

The normalized correlation coefficient  $C_{12}(x_o, y_o; P)$  has a maximum value of unity when  $t_1(x, y)$  is a constant times  $t_2(x+x_o, y+y_o)$  over the correlation area. Since  $t_1$  and  $t_2$  can differ within a multiplicative constant, it is seen that different exposure levels for the two transparencies are of no consequence.

In practice the amplitude transmittance of the two transparencies should be represented as

$$t_1(x, y) = t_{01} + t'_1(x, y)$$

and

$$t_2(x, y) = t_{02} + t'_2(x, y)$$

where  $t_{01}$  and  $t_{02}$  represent the average transmittance and  $t'_1(x, y)$  and  $t'_2(x, y)$  represent image structure information. The presence of terms  $t_{01}$  and  $t_{02}$  do not affect the final value of the normalized correlation coefficient.

However the amplitude of the a. c. signal given by equation (2.9) becomes

$$\begin{aligned}
 S_V(P) &= 2K \iint t_{01} t_{02} + t_{01} t'_2(x+x_o, y+y_o) + t_{02} t'_1(x, y) \, dA \\
 &\quad + 2K \iint t'_1(x, y) t'_2(x+x_o, y+y_o) \, dA \\
 &= S_{VO}(P) + S'_V(P).
 \end{aligned} \tag{2.13}$$

$S_{VO}(P)$  represents a constant amplitude a. c. signal and  $S'_V(P)$  represents the correlation signal whose amplitude depends on the correlation between the two transparencies. In practice the changes in  $S'_V(P)$  are very small compared to the magnitude of  $S_{VO}(P)$  and hence the measurement problem becomes complicated due to the limited dynamic range of the photodetector array to be used. This problem is overcome by putting d. c. blocks at the back focal plane of the imaging lenses as illustrated in Figure (2.1). The d. c. blocks in effect remove the terms  $t_{01}$  and  $t_{02}$  and the amplitude of the a. c. signal directly represents the correlation amplitude.

Now let us consider the correlation signal amplitude given by equation (2.9)

$$S_V(x_o, y_o; P) = 2K \iint t_1(x, y) t_2(x+x_o, y+y_o) \, dA.$$

Other correlation schemes have relied on the selection of the maximum value of  $S_V(x_o, y_o; P)$  or its one-dimensional form to determine conjugate image coincidence at point P. Unlike the normalized correlation

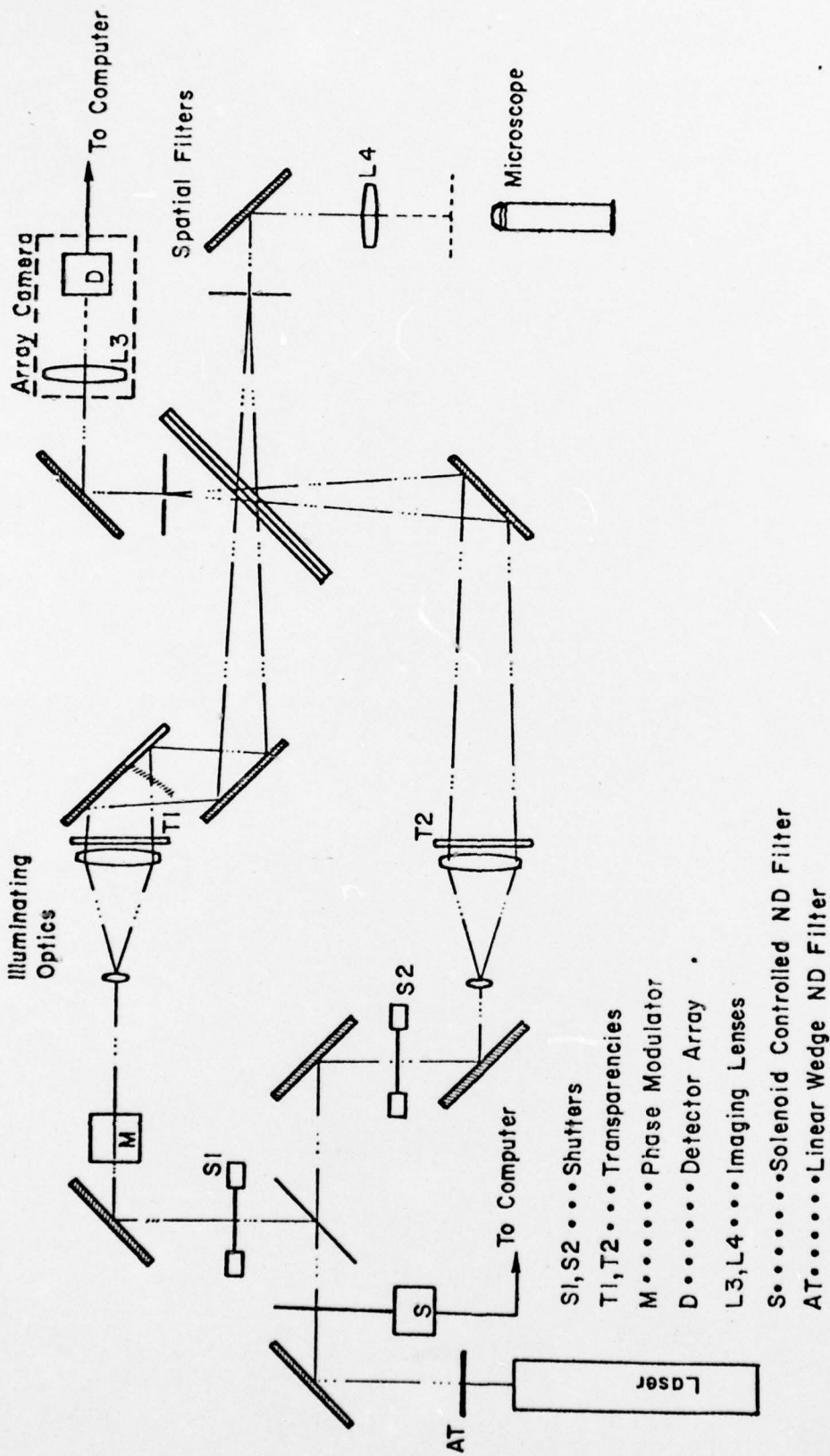


Figure 2.2 Experimental HOC System

coefficient  $C_{12}(x_o, y_o; P)$ ,  $S_V(x_o, y_o; P)$  has no unique maximum value and its value is dependent on the average transmittance of  $t_1(x, y)$  and  $t_2(x, y)$ . Hence the selection of a local maximum can lead to false correlation. This is one of the reasons why all the electronic correlation systems as well as some of the optical correlation systems rely on tracking to avoid ambiguity. Tracking assumes that the conjugate images are always within the proximity of coincidence.

Theoretically the normalized correlation function  $C_{12}(x_o, y_o; P)$  monotonically decreases when the magnitude of the displacement vector  $(x_o, y_o)$  is increased. The derivatives of the normalized correlation function depend upon image structure and the contrast of the image being correlated. The slope of the normalized correlation function also determines the accuracy of parallax measurement. By determining the displacement  $(x_o, y_o)$  necessary to achieve a maximum value for the normalized correlation coefficient it is possible to determine the parallax difference associated with the image point P.

### 2.3 Experimental HOC System

The experimental HOC System was designed and fabricated with the objective of determining the feasibility of the heterodyne optical correlation concept. The optical configuration of the experimental HOC system is shown in Figure 2.2

Light from the laser (Spectra Physics Model 125-50 mw) is directed into the two channels of the interferometer with the 50/50 dielectric beam splitter. A linear wedge neutral density filter permits attenuation of the laser power before it enters the interferometer. Electronically operated shutters  $S_1$  and  $S_2$  permit selective illumination of the two transparencies. The modulator M is used to modulate the optical path difference between the two channels of the interferometer. The modulator consists of a 5x5x1 mm size glass plate

attached to the spindle of a Galvoscanner (General Scanning G-100) . The oscillation of the glass plate in the path of the beam results in the time modulation of the optical path difference between the two beams.

The illuminating optics in each channel of the interferometer consists of a beam diverger and a condenser. The standard microscope objective (20X) and a spatial filter placed at its front focal point make up the diverging optics. The condenser consists of a combination of two collimating objectives mounted back to back so as to minimize wavefront distortion. The objectives have focal lengths of 220 and 540 mm and both lenses have clear aperture diameters of 50 mm. The two transparencies  $T_1$  and  $T_2$  are mounted on translation stages and are placed as close to the condenser optics as possible so as to obtain maximum coverage of the area of illumination at the plane of transparency. The circular illumination area obtained in the experimental HOC has a diameter of approximately 40 mm.

The final imaging lens  $L_3$  (EL NIKKOR Projection Lens, 85mm/f2.8) produces superimposed images of the transparencies at the common image plane occupied by the detector array. The beam splitter, acting as a tilted plane parallel glass plate introduces astigmatic aberration in the imaging process. However since the beam splitter is located at the long conjugate side of the imaging lens ( $f^\#$  of the cone of rays being large), the aberration introduced is negligible. The beam splitter is formed by cementing together two identical plane parallel glass plates with the beam splitting coating at the cemented interface. This symmetric nature of the final beam splitter also assures that the aberrations have the same effect on both images. Thus the aberrations produced have little effect on the correlation value.

The d. c. block is a circular opaque spot (.25 mm diameter) formed with India Ink on a microscope slide and is placed at the point of convergence

of the illuminating beam. The d. c. block is located between the final beam splitter and the imaging lens  $L_3$  and hence is common to both images. Because of this fact once again the small aberration contribution of the microscope slide has negligible effect on the correlation value. It is to be emphasized here that minimum number of optical components have been introduced between the transparencies and the final imaging lens. This simplicity in optical configuration not only enhances the resolution performance of the final imaging optics but also reduces significantly geometric distortions during imaging. Hence it is possible to maintain the geometric fidelity of the transparencies during the measurement process.

The final beam splitter has two output beam paths that are normal to each other. One of the beam paths as described earlier is directed to the array detector. Lens  $L_4$  (EL NIKKOR Projected Lens 85mm f/2.8), placed symmetrical to lens  $L_3$  in the path of the other beam also produces superimposed images of the transparencies in the common image plane. The common image is examined under white light illumination with a 100X microscope mounted on a three axis stage. The visual examination of the common image plane permits manual relative orientation of the two transparencies.

The mechanical part of the system consists of the various translation stages containing the transparencies, the array camera and the microscope, mechanical mounts for lenses, mirrors and beam splitters and the overall support for the instrument. In this section no detailed description of the mechanical mounts is provided for the sake of brevity. The fundamental requirement of the mechanical mounts used in the system is mechanical rigidity. Each transparency is mounted in the plate holder, its face against a plane steel reference surface as a reference for the instrument. The holder is mounted on a three-axis translation stage, each axis being controlled independently by a stepping motor, having an incremental resolution of 3.175

micrometers. The plate holder can also be rotated about the optical axis of the system (normal to its plane) with a resolution of about 40 arc secs. During the initial mechanical alignment of the system the steel reference surfaces are made parallel to within a few minutes of arc. The microscope stages and the array camera stages are mechanically aligned to be parallel to the stages containing the transparencies and hence reference points can be transferred easily from one coordinate system to the other provided the magnification between stages is known exactly (as discussed later in this report, the magnification can be measured very accurately). The stages are mounted to the main frame rigidly to provide a high degree of repeatability and stability.

The electronic system consists of the detector array and its interface electronics, the shutter controls, the stepping motor controls and the control computer. The array used is a 32x32 element RETICON array. The array is interfaced directly to the control computer so that the output of each element can be read sequentially. The saturation exposure for the array is  $3 \mu \text{w/cm}^2 \text{ sec}$ . The sensitivity of the detector depends upon the integration time (time to scan a complete frame) and it can be altered by altering the clock frequency. The smaller the clock frequency the greater is the sensitivity of the detector. However the smaller the clock frequency depends upon the power density available at the final image plane.

In the present HOC system a 200 KHz clock rate was used resulting in an integration time of 5.12 msec. Power density for saturation was approximately  $0.6 \text{ mw/cm}^2$ . Because of the large power He-Ne laser that was used in the experimental HOC, it was necessary to lower the laser power input with neutral density filters to achieve a power density lower than the saturation level. In the case of the experimental HOC the clock rate was optimized on the basis of the input/output requirements of the control computer.

The shutters (VINCENT ASSOC) are operated directly by the control computer and have a time of response of about 5 msecs. Each of the stepping

motors associated with the six stages (three for each of the transparencies) can be independently controlled by the computer. The modulator's Galvo-scanner is driven by an independent signal source and is not controlled by the computer. In order to minimize the dynamic range and nonlinear problems associated with the array due to the fourfold increase in maximum output, when both shutters are open, a neutral density filter operated by a solenoid mechanism is introduced into the path of the laser beam before it enters the interferometer. The neutral density filter is inserted only when both shutters are open and its operation is also controlled by the control computer. The control computer used is a HP21MX minicomputer with a 24K memory.

#### 2.4 Stereo Compilation Procedure

This procedure refers to the actual measurement of  $x$  and  $y$  parallaxes between conjugate images in a stereopair of transparencies. The measurement procedure of the experimental HOC can be considered identical to stereocomparator measurements at a two-dimensional matrix of points defined by the projections of the detector array. Because of the extreme geometric fidelity of the detector array, each elemental area defines a precise location on the transparency.

By using a grid plate for initialization, it is possible to relate precisely the coordinate system of the array elements to that of the photostages. The procedure for compiling a stereomodel is as follows: with the use of the microscope, the two transparencies representing the model are relatively oriented and the  $x$ -parallax direction is made to correspond to the  $x$ -axis of the translational stages. Once the relative orientation of the stereo transparencies in the instrument has been achieved, the starting point for the compilation procedure is the adjustment of the movable transparency in Channel 1 to represent conjugate image coincidence in a chosen datum plane (to assure  $x$  and  $y$

axes translation along one direction). These operations have been accomplished with white light, hereafter coherent light is used.

For any given orientation of the two superimposed images the normalized correlation coefficient is determined at each element of the array. To accomplish this, the values corresponding to Equation (2.10) and (2.11) are first determined for individual projectors, by measuring the intensity distribution over the image plane due to each projector when the light from the other projector is blocked. The modulated intensity value defined by Equation (2.8) is then determined. In actuality this sequence of steps is automatically carried out by the control computer. First with shutter in Channel 1 closed, the output of each element of the array is read and stored in the computer. In order to improve the signal to noise ratio, the average of the readings of several frames is made. The number of frames to be averaged (five in most of the experiments performed is one of the input parameters and can be adjusted to be any value greater than zero. The number of frames to be averaged is optimized against the required speed of the compilation procedure. The same procedure is repeated with the shutter in Channel 1 closed. Finally the modulated intensity term is determined with the shutter in both channels open. Due to the interference between the two beams, the intensity distribution at the image plane is time modulated at the frequency determined by the modulator in Channel 1 of the interferometer. During this measurement, the output of the array is read sequentially over several frames. The first reading is stored in two locations to represent the minimum intensity and the maximum intensity corresponding to each element of the array. The output of the subsequent frames is compared to the maximum and minimum values stored for the corresponding element and the resulting maximum and minimum values are stored. After a large number of frames compared to the frequency of modulation has been read, the difference between the stored maximum and minimum intensity

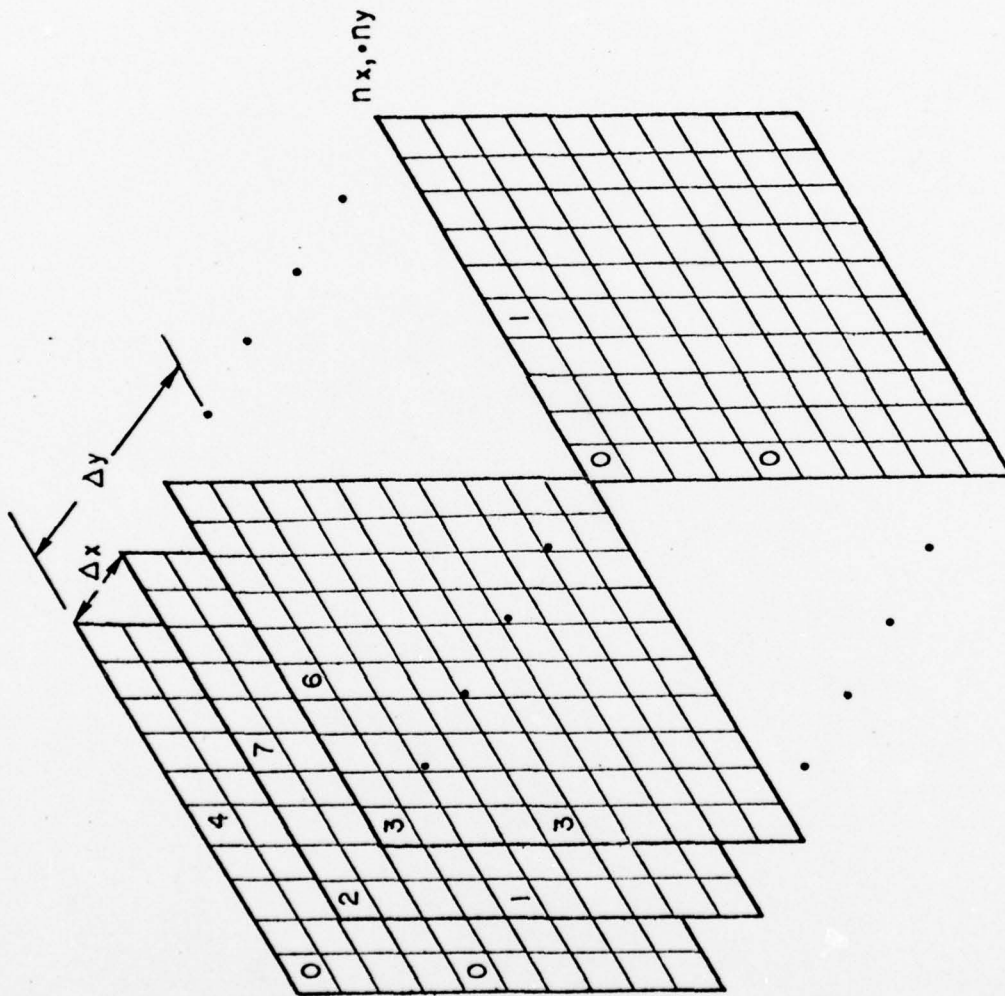


Figure 2.3 Correlation Coefficient Data Matrix

values provides the amplitude defined by the Equation (2.5) for each element of the array. The increase in the number of frames read decreases the uncertainty in the measurement of the amplitude of modulated intensity, however it has to be optimized against the speed of operation. The number of fringe sampling frames used in most of the experiments is 32 and its value can be adjusted. The number of frames averaged and the number of fringe sample frames are a part of the input parameters to the control computer.

The computer introduces the x-parallax steps in incremental fashion and the normalized correlation value at each element of the array at each step is determined and stored. After the prescribed number of x-parallax steps, the x-stage returns to the original position. Next a y-parallax step is introduced. The stepping in x-parallax is repeated for the new y-parallax position. The procedure is repeated for the prescribed number of y-parallax positions. The total number of steps taken is given by  $n_x n_y$  where  $n_x$  is the number of x-parallax steps and  $n_y$  is the number of y-parallax steps. The resultant data can be represented in a three-dimensional form shown in Figure 2.3. It is clear that by scanning the histogram of the normalized correlation values, it is possible to determine, for any given element on the array, at what x and y step the image matching was maximum. Hence x and y step values at which image matching was maximum becomes the x and y parallax value for the correlation area defined by that element on the reference transparency. The final output of the computer is then two 2-D matrices of x and y parallax values representing each elemental area defined by the array (Figure 2.4). During actual measurement the three-dimensional matrix illustrated in Figure 2.3 is never stored. For a given x and y parallax position, the output of the measurement sequence provides three parameters for each element of the array. They are the x and y parallax steps and the corresponding normalized correlation coefficient.

$P_{x_{11}}$	.	.	.	$P_{x_{55}}$	.	.	.	.	$P_{x_{1010}}$
.	$P_{x_{22}}$								
.		.							
.			.						
$P_{x_{55}}$				.	.				
.					.				
.						.			
.							.		
.								.	
$P_{x_{1010}}$									.

$P_{y_{11}}$	.	.	.	$P_{y_{55}}$	.	.	.	.	$P_{y_{1010}}$
.	$P_{y_{22}}$								
.		.							
.			.						
$P_{y_{55}}$				.	.				
.					.				
.						.			
.							.		
.								.	
$P_{y_{1010}}$									.

Figure 2.4 Parallax Matrix Output

The value of the normalized correlation coefficient is compared with the previous stored value for the corresponding array element and only the parameters corresponding to the maximum value are stored. Thus the storage requirement for the control computer is greatly reduced. The storage requirement is determined by the array size and not by the number of  $x$  and  $y$  parallax steps introduced.

The objective of the experimental HOC tests were to demonstrate the feasibility of the concept. Hence the problem of measurement, storage and manipulation of the data was simplified by restricting the measurement to  $x$ -parallax values. However the  $y$ -parallax steps were still necessary to maximize correlation and unambiguously define the  $x$ -parallax value and the exact  $y$ -parallax step value was neither tracked nor stored. Since most of the aerial transparencies used during the tests were nearly vertical, the  $y$ -parallax values were small and did not introduce significant errors. Also this compromise in measurement reduced the need for additional computer memory.

When there is insufficient image structure present within the correlation area of either of the transparencies, the image intensity measurement of the corresponding detector element will be a minimum due to the presence of the d. c. block in front of the imaging lens. Image structure is necessary to diffract light beyond the d. c. block in the spatial filter. To avoid ambiguous correlation due to noise, in such cases, a condition on the minimum value for the intensity measurement can be imposed. Only measurements greater than this threshold are considered for further computation of the correlation coefficient for that particular element. In the experimental HOC such areas are delineated by the presence of zeros in the final output for the parallax values.

## 2.5 Summary

In this chapter a brief introduction to the concept of Heterodyne optical correlation has been presented along with the description and the operation

of the experimental HOC system. The purpose of this chapter is to provide continuity to the report and more detailed discussions on the text and evaluation of the experimental system can be found in references (2, 3 ).

### 3 PROPOSED PROTOTYPE SYSTEM MODEL

#### 3.1 Introduction

The experimental HOC System described earlier was designed and fabricated to demonstrate the feasibility of the HOC concept under conditions of real world aerial imagery. During its design no considerations were made to optimize the system configuration and the measurement procedure. Hence the configuration of the experimental HOC system does not necessarily represent the optimum configuration for a prototype system. The prototype system model chosen has a definite bearing on the feasibility and applicability of the prototype HOC system for field applications. The heterodyne optical correlation system is a generalized optical correlation system which permits the detection of coincidence of conjugate images in a superimposed common image plane. In general the HOC system is a complex optomechanical and optoelectronic instrument. The nature of the operating conditions and requirements determine the complexity and the interaction between the various subsystems. Hence in reality the prototype HOC system model should be developed after considering the effects of the operating environment on performance. In this study a system model is first developed on the basis of first order evaluation and interaction of system requirements. The feasibility and applicability of the proposed system for field applications is then evaluated. Finally a design of potential prototype system is described along with its tolerance requirements. In this chapter, the evolution of the HOC system model is presented along with its advantages and disadvantages. The unique characteristics of the proposed system model are also outlined.

#### 3.2 System Requirements

The intended application of the HOC system is for a prototype van-mounted stereomodel digitizer to be used in the field. The requirements for the proposed stereo model digitizer are

- (a) the instrument should be capable of generating digital terrain model automatically and output the data onto magnetic tape. The spatial and height resolution of the output data must be such as to meet the needs of an off-line orthoprinter,
- (b) the instrument should be capable of handling small scale metric quality frame photos as input. The applicability of the instrument to other formats such as oblique and panoramic inputs should be considered,
- (c) the accuracy of the digital terrain model measured must be such that 90% of the points at orthoscale (1:12,000) should be within 1/30th of an inch of the measured point,
- (d) the instrument should be rugged enough to withstand on and off road movements in a van and yet simple in construction. Operator skill required and interaction should be kept to a minimum. Finally the speed of operation of the instrument is less significant but it must be consistent with the reduced requirements on accuracy for this instrument.

The system requirements outlined above clearly indicate that if the HOC system were to be applicable it must be capable of withstanding adverse environmental and operating conditions. While in concept the HOC system can meet the performance requirement (a) and (c), the system model chosen will determine the capability with regards to performance requirement (b) and (d).

### 3.3 System Model Options

There are several options available for HOC system configuration and the measurement procedure. The HOC system can be configured analogous to a double projection, photogrammetric plotting instrument or a stereo comparator -

analytical plotter. Also depending upon the input photogeometry, either the entire model can be compiled in one stage or the model can be compiled in small sections.

Following an earlier investigation of the performance of the experimental HOC system, the design for a follow-on prototype HOC system configuration was described. The optical configuration of the proposed system is shown in Figure 3.1. The salient characteristics of the proposed system are:

- (a) a two-dimensional detector array of 320x512 elements covers the entire overlapping areas of the two transparencies,
- (b) the total translation of the movable transparency is limited to the maximum anticipated parallax in X and Y directions,
- (c) except for the condensing lenses all the optical components used are relatively small in size. This characteristics permits the overall system to be small and compact and hence rigid and mechanically stable,
- (d) the HOC system output gives the x and y parallax distribution over the stationary control transparency and must be digitally converted to provide the digital terrain values,
- (e) the system operates on the entire model area in parallel, depending on array and computer interface electronics, the system is capable of increased operational speed.

In the HOC system model, by opting to cover the entire model area in one step, the mechanical problems of translation of the transparencies have been greatly minimized. However consider the following data handling problems. In order to compute the normalized correlation co-efficient at every element on the detector array for any given parallax position, the

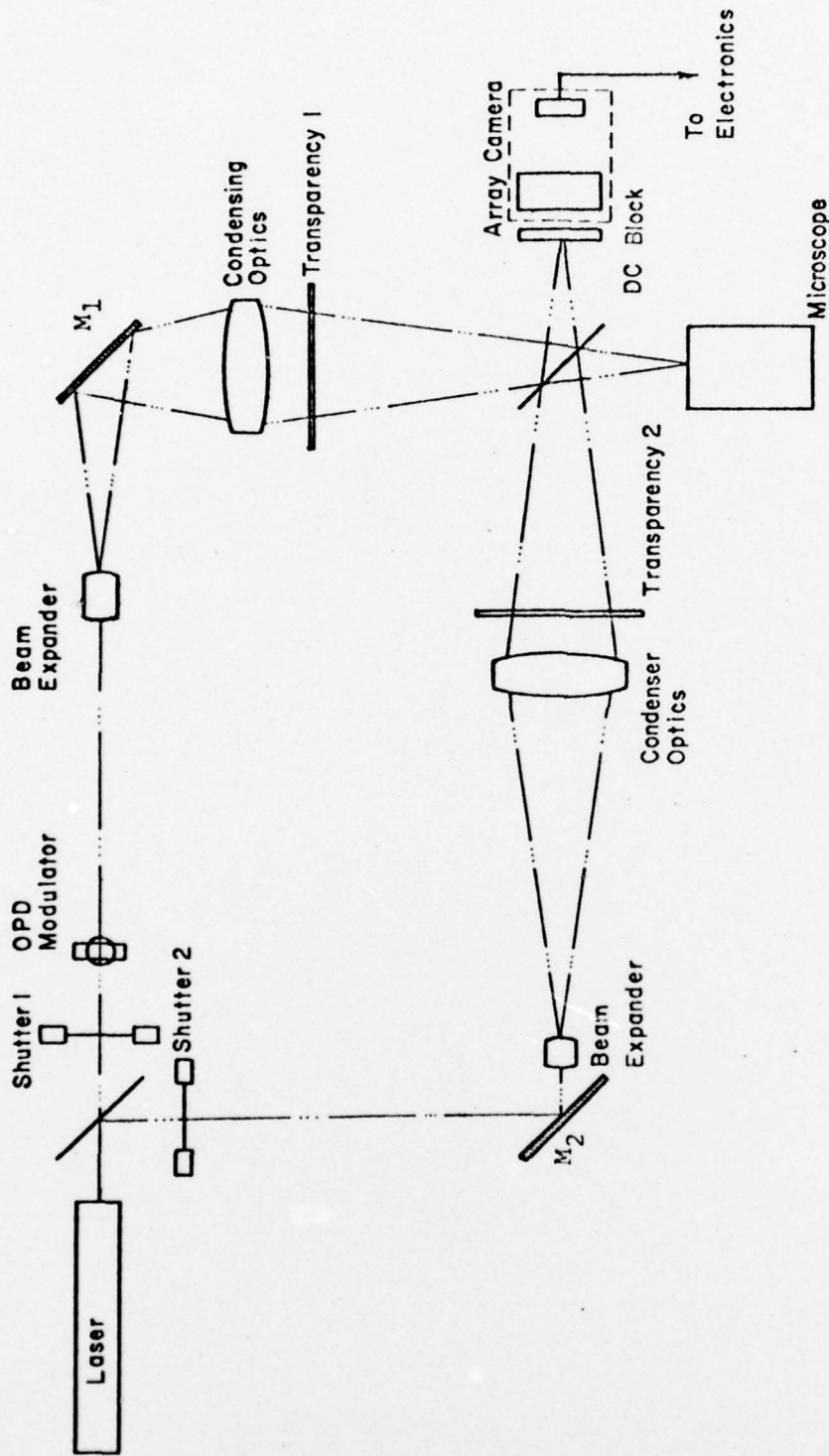


Figure 3.1 Prototype HOC System

number of data points to be stored is  $8 \times 320 \times 512$  eight bit words. That represents over 10 megabits. This requirement for large memory along with problem of data handling result in insurmountable problems. Thus while, the instrument is compact and simple from an opto-mechanical point of view it becomes very complex and slow considering digital data handling and data management problems. These factors complicate the concept of the prototype HOC as a compact and simple stand alone instrument. These arguments formed the basis for the rejection of this system model for the HOC prototype.

Consider now the model in which only a small area (2.5 cm square) on the plane of the transparency is illuminated at any instant. Hence the large condenser lens shown in Figure 3.1 can now be replaced by a one inch diameter collimator lens. The illuminated areas on the plane of the transparencies are imaged onto a small  $50 \times 50$  detector array instead of  $320 \times 512$  detector array. The two transparencies are mounted such that they can be moved together such that any portion of the overlapped area between the transparencies can be covered by the illuminating 2.5 cm square aperture. The transparency 2 is in turn mounted on a small stage which permits only small relative translation of transparency 2 with respect to transparency 1. This small x and y translation is necessary to introduce the parallax during measurement.

In this HOC system model configuration only a small area is illuminated at any given time. This reduces the complexity of the optics used and also the over all optical length can be made small. All these factors permit the optical system to be small, compact and hence highly stable. From an electronic data processing point of view, at any given instant data corresponding to only 2500 points are being manipulated to arrive at the parallax value and hence the memory and processing hardware requirements are small. It is highly probable that the requirements can be handled by microprocessor based systems.

In this HOC system model the electronic data reduction and handling hardware problems have been overcome at the expense of simplicity and the non-kinematic aspects of large mechanical components. Since the formats of the transparencies to be handled by the system are large, large displacements are involved in moving the transparencies over the illuminated area to cover the entire stereo model. However by decoupling the parallax measurement stage from that of the image scanning stage, the problem of obtaining high precision and accuracy of displacement over fairly large distances is greatly reduced. Any errors that result during the image scan motion reflect as registration errors between different blocks of points compiled independently and they do not reflect in the accuracy of parallax measurement. Only the second translation stage (which has only limited travel) has to be very accurate, since its displacements, directly represent parallax. Thus by proper trade off between the optical, mechanical and electronic subsystems it is possible to configure an HOC system that meets the objective.

From a photogrammetric data reduction point of view, there is again a trade off between optical system complexity and electronic data processing hardware requirements. The HOC instrument can be considered a double projection system in which the individual transparencies can be relatively oriented to provide an image at the common image plane that is corrected for scale, tilt and tip. This approach minimizes the subsequent photogrammetric manipulation of the data measured. However the requirements for change in scale, tilt and tip put a great demand in the stability and flexibility of optical and mechanical components.

However if the transparencies were mounted such that they are parallel to the output array plane then the data extracted from the HOC becomes essentially those obtainable from a stereo comparator. This is because of

the fixed relationship between the reference transparency and the detector array and the definition of the co-ordinates of the conjugate image points in the movable transparency 2 through the measured x and y parallax data. The measured data have to be subsequently processed to produce the object space co-ordinate information.

By adopting the small detector array approach the on-line photogrammetric processing of the measured data to produce ground positional information becomes feasible and attractive. This approach to HOC measurement procedure is not without its limitations. These limitations will be discussed in detail later in this report.

The proposed HOC system model is illustrated in Figure 5.2. The general characteristics of the proposed system are:

- (a) The illuminating beam diameters at the plane of the transparency is 1.5 inches. A 50x50 detector array projected back onto the transparency covers a square inch area.
- (b) The plane of the transparencies are fixed with respect to the imaging optics and the detector array and are projected on the array plane at nominally the same scale. The plane of the transparencies as well as the plane of the detector array are perpendicular to the optical axis of the imaging lens.
- (c) A large stage on which the two transparencies are mounted permit the translation of the two transparencies together to cover the entire stereo model area. A small stage mounted on top of the large stage permits translation of transparency 2 with respect to transparency 1 so as to introduce parallax during measurement. The stages are all mounted horizontally to assure mechanical stability and speed of translation.

- (d) Independent processing hardware permits continuous processing of the measured data in 50x50 blocks to obtain digital terrain data. This factor overcomes the need for bulk data handling.

Based on this system model the feasibility of the HOC system as a van mounted stereomodel digitizer is evaluated in the following pages of this report.

## 4 HOC SYSTEM EVALUATION

### 4.1 Introduction

In order to assess the feasibility and applicability of the HOC system for field applications, the tolerance specifications of the optical, mechanical and electronic subsystems as a function of the required performance characteristics of the system must be evaluated. In this chapter the characteristics and tolerances of the various components and subsystems that form the potential HOC system are evaluated from the point of view of fabrication and maintenance.

### 4.2 Effects of Vibration on Correlation Co-Efficient Measurements

The measurement of the normalized correlation co-efficient  $C_{12}$  forms the basis for detecting conjugate image coincidence in a HOC system and hence any errors in its measurement directly affects the accuracy and precision of the  $x$  and  $y$  parallax measurements. One of the major environmental factors that is important from the point of view of correlation co-efficient measurement is mechanical vibration of the optical system. Vibration problems associated with optical systems have always been a source of concern and the HOC system being an interferometer is highly susceptible. There are basically two approaches to overcome the vibration problems. First the instrument can be made extremely rigid mechanically but such an approach would make the over all optical subsystem heavy, large and cumbersome. The second approach is to make the measurement process relatively insensitive to typical mechanical vibration likely to be encountered in a field application.

In the experimental HOC, during the correlation co-efficient measurement, the values corresponding to equations (2.10) and (2.11) are first determined for individual projectors by measuring the intensity distribution over the image plane due to each projector when the light from the other projector

is blocked. During this measurement process mechanical displacements due to typical vibration do not cause any problems. After these measurements the modulated intensity value defined by equation (2.9) is then determined. During this measurement the array is read sequentially over several frames. Due to the interference between the two beams, the intensity distribution at the output image plane is time modulated at the frequency determined by the modulator in channel 1 of the interferometer. The scanned data from the array is searched to determine the maximum and minimum values at each element of the detector array. The peak to peak value of the intensity fluctuation can then be used to define the amplitude given by equation (2.9). The increase in the number of frames scanned decreases the uncertainty in the measurement of the amplitude defined by equation (2.9) and hence reduces the uncertainty in the measurement of the normalized correlation co-efficient. Since this measurement process occurs over nearly one to two seconds, any modulation of the fringe pattern due to vibration interferes with the measurement process. Hence the experimental HOC measurement approach used as such would represent an operational draw-back.

However modifications to the measurement approach are feasible that permit one to overcome these problems. Consider the following measurement process in which four measurements of the intensity distribution at the common image plane is made using the detector array.

- Measurement 1( $I_1$ ): Array reading with one channel of the interferometer closed (channel 2)
- Measurement 2( $I_2$ ): Array reading with both channels of the interferometer open
- Measurement 3( $I_3$ ): Array reading with both channels open and one channel phase shifted by  $90^\circ$

- Measurement 4( $I_4$ ): Array reading with both channels open and one channel phase shifted by an additional  $90^\circ$
- Stored Value ( $I_0$ ): The dark current measured with both channels closed at the start of the measurement procedure.
- transparency 1 in channel 1:  $t_1(x, y)$
- transparency 2 in channel 2:  $t_2(x, y)$

A is the projected area of the individual detector at the plane of the transparency.

$$I_0 = \text{Dark Current} \quad (4.1)$$

$$I_1 = \int t_1^2 dA + \text{dark current} \quad (4.1)$$

$$I_1 = \int t_1^2 dA + I_0$$

$$I_2 = \int t_1^2 dA + \int t_2^2 dA + 2 \cos k\Delta \int t_1 t_2 dA + I_0 \quad (4.2)$$

$$I_3 = \int t_1^2 dA + \int t_2^2 dA - 2 \sin k\Delta \int t_1 t_2 dA + I_0 \quad (4.3)$$

$$I_4 = \int t_1^2 dA + \int t_2^2 dA - 2 \cos k\Delta \int t_1 t_2 dA + I_0 \quad (4.4)$$

$$\int t_1^2 dA = I_1 - I_0 \quad (4.5)$$

$$\int t_1^2 dA + \int t_2^2 dA = \left[ \frac{I_2 + I_4}{2} - I_0 \right]$$

$$\int t_2^2 dA = \left[ \frac{I_2 + I_4}{2} - I_1 \right]. \quad (4.6)$$

$$\begin{aligned}
 2 \operatorname{sinc} k\Delta \int t_1 t_2 dA &= \left[ \frac{I_2 + I_4}{2} - I_0 \right] - \left[ I_3 - I_0 \right] \\
 &= \left[ \frac{I_2 + I_4}{2} - I_3 \right].
 \end{aligned} \tag{4.7}$$

$$2 \cos k\Delta \int t_1 t_2 dA = \left( \frac{I_2 - I_4}{2} \right) \tag{4.8}$$

$$\begin{aligned}
 \left| \int t_1 t_2 dA \right|^2 &= 1/4 \left[ \left[ \frac{I_2 + I_4 - 2I_3}{2} \right]^2 + \left[ \frac{I_2 - I_4}{2} \right]^2 \right] \\
 &= 1/16 \left[ (I_2 + I_4 - 2I_3)^2 + (I_2 - I_4)^2 \right]
 \end{aligned} \tag{4.9}$$

The correlation coefficient  $C_{12}$  is given by

$$\begin{aligned}
 |C_{12}|^2 &= \frac{\left| \int t_1 t_2 dA \right|^2}{\int t_1^2 dA \int t_2^2 dA} \\
 &= 1/16 \left[ \frac{(I_2 + I_4 - 2I_3)^2 + (I_2 - I_4)^2}{\left[ \frac{I_2 + I_4}{2} - I_1 \right] \left[ I_1 - I_0 \right]} \right]
 \end{aligned} \tag{4.10}$$

for the purpose of determining the location of image co-incidence  $|C_{12}|^2$  is as good as  $C_{12}$ .

In this measurement process the intensity distribution at the image plane can be stable during the four measurements with the detector array. With a 50x50 detector array operating at a clock frequency of 400 KHz, the time required to make the measurement is about 25 msec. Most of the mechanical vibrations are about 10-15 Hz and hence for all practical purposes the intensity distribution is stable during the measurement process.

Experiments were performed with the experimental HOC at the Center for Coherent Optics, USAETL, to prove the feasibility of the new measurement process. The comparison of the correlation values measured using the new measurement approach and the old approach proved the feasibility and indicated that the measurement speed is limited by the computer rather than by system inertia. The new measurement approach not only makes feasible the application of the HOC instrument under reasonably hostile vibration environment, but, as discussed later, represents a significant improvement in the evolutionary development of the HOC prototype system.

#### 4.3 Effects of Mechanical and Thermal Drifts or Normalized Correlation Coefficient Measurement

The determining of the optical system and the interferometer is a realistic possibility in the application HOC type instrument in a field environment. The stability of optical alignment is of concern in four sections of the HOC optical configuration. They are (1) Beam expanding optics, (2) Condensing optical system, (3) Imaging optics and (4) the Interferometer.

The stability problems associated with the first three are less significant while the stability problems of the interferometer has direct consequence on the measurement process. The effect of stability (both laser beam and optics) on the beam expanding optics is to destroy the uniform illumination across the beam diameter. This problem as it applies to the HOC system can be overcome

by proper design of the beam expanding optics. For example by making the spatial filter pinhole to be of slightly larger diameter than the diffraction limited spot, the sensitivity of the beam expanding optics to stability problems can be reduced.

The concern for the condensing optics stability is caused by the requirement of the relative alignment between the d. c. block in front of the imaging optics and the optical axis of the condenser. By making the size of the d. c. block slightly larger than the diffraction limited spot size of the condenser lens, the critical alignment requirement can be reduced. The d. c. block can not be made excessively large since that would not only reduce the power at the common image plane but also remove the low spatial frequency information from the transparencies. However by proper choice of the focal length of the condensing optics and the size of the d. c. block this problem can be overcome.

The stability of the imaging optics deals directly with the registration of the array with respect to the coordinate system of the transparencies. Anticipated drift problems would cause only very minor error in registration and even some of these errors can be reduced by subsequent processing of the final digital terrain model data.

Any misalignment of the interferometer due to thermal or mechanical drifts alters the shape and spacing of the interferometric fringes produced in the final image plane. According to the conditions defined by equation (2.8), the optical path difference between the interfering beams over the individual detector element is essentially a constant. The thermal and mechanical instabilities invalidate this assumption that  $\Delta_o(x, y)$  is a constant over the aperture  $A$  of the detector element. However if the aperture diameter of the detector  $A$  is still small compared to the fringe spacing, then the path difference distribution can be written as

$$\Delta_o(x, y) = \Delta_o + \delta(x, y)$$

where  $\Delta_o$  is a constant over  $A$  representing the average value and  $\delta(x, y)$  is the variation about  $\Delta_o$ . When the width of the detector is small compared to the fringe spacing  $\delta(x, y)$  is small. Equation (2.8) now becomes

$$S_V(P, t) = 2K \iint t_1(x, y) t_2(x+x_o, y+y_o) \cos \frac{2\pi}{\lambda} (\Delta_o + \delta(x, y) + Vt) dA \quad (4.11)$$

$$\begin{aligned} \cos \frac{2\pi}{\lambda} (\Delta_o + Vt + \delta(x, y)) &= \cos \frac{2\pi}{\lambda} (\Delta_o + Vt) \cos \frac{2\pi}{\lambda} \delta(x, y) \\ &\quad - \sin \frac{2\pi}{\lambda} (\Delta_o + Vt) \sin \frac{2\pi}{\lambda} \delta(x, y) \\ &= \cos \frac{2\pi}{\lambda} (\Delta_o + Vt) \left[ 1 - \frac{\left( \frac{2\pi}{\lambda} \delta(x, y) \right)^2}{2} \right] \\ &\quad - \sin \frac{2\pi}{\lambda} (\Delta_o + Vt) \cdot \frac{2\pi}{\lambda} \delta(x, y) \end{aligned}$$

neglecting higher order terms.

Equation then becomes

$$\begin{aligned} S_V(P, t) &= 2K \cos \frac{2\pi}{\lambda} (\Delta_o + Vt) \iint_A t_1 t_2 dA \\ &\quad - \frac{2\pi}{\lambda} K \cos \frac{2\pi}{\lambda} (\Delta_o + Vt) \iint_A t_1 t_2 \delta^2(x, y) dA \\ &\quad - \frac{4\pi}{\lambda} K \sin \frac{2\pi}{\lambda} \iint_A t_1 t_2 \delta(x, y) dA. \end{aligned} \quad (4.12)$$

The above expression shows that the effects of interferometer misalignment is to lower the value  $S_V(P, t)$  and hence the value of  $C_{12}$ . As long as the value

of  $\delta(x, y)$  is small the reduction in the value of  $C_{12}$  has no significant impact in the measurement process since only the relative value of  $C_{12}$  is important.

To obtain a qualitative idea of the tolerances involved consider the following numerical example.

Total area of the image covered on the plane of the transparency is one square inch and the size of the array used is 50 x 50. It can be shown that the assumption  $\frac{2\pi}{\lambda} \delta(x, y)$  is small, is valid when ever the detector aperture is about 1/5th the period of the fringe pattern. Hence there can be as many as 10 fringes within the image area.

The angular tilt of the plane wave

$$\begin{aligned} &= \frac{10 \times \lambda/2}{25 \text{ mm}} \quad (\lambda \approx .6 \text{ microns}) \\ &= .012 \text{ radians} \\ &= .7 \text{ degrees or } 42 \text{ minutes.} \end{aligned}$$

This angle is large for an optical system. This calculation not only shows that the system is not as sensitive to mechanical and thermal drifts as a conventional optical interferometer but also the wedge angles associated with the film substrates will have minimal effect on the measurement process as long as they are of reasonable quality. (For example ordinary plate window glass has the tolerance of 1-2 fringes/inch variation on the wedge angle.)

#### 4.4 Tolerance Requirements of Translation Stages and their Effect on Measurement accuracy

In the proposed HOC system the option of mechanical translation of the transparencies over the illuminated aperture of the interferometer was selected to minimize the data reduction and data handling hardware problems.

Earlier in Chapter 3 it was stated that by decoupling the parallax stage and the image scanning stage, the problems of obtaining high precision and accuracy of displacement over large distances is greatly reduced. In this section detailed explanation is presented to show that the tolerance requirements on the translation stages are not severe. The requirements for precision and accurate translation stages would be a disadvantage for HOC as a field instrument, since such stages require continuous care and maintenance.

The tolerance requirements for the translation stages can be illustrated by considering the operation of the HOC system with 9" frame inputs. Typical correlation area on the plane of the transparency is 500x500 micrometers and hence a 50x50 detector array covers a 1x1 inch square on the transparency. During the parallax measurement phase, the movable transparency is translated with respect to stationary reference transparency in both x and y directions. The maximum translation requirement of the parallax stage in both x and y directions is approximately an inch. The accuracy and precision of the magnitude of the parallax measured is entirely determined by the parallax stage. It is comparatively easy to obtain high accuracy and precision (of the order of a micron) in stages that have a total translation of an inch. Typically there may be 50 square inches in a square model and hence the large translation stage permits simultaneous displacement of the two transparencies and the parallax to permit measurement in the adjacent square inch area. The total translation requirements for the large x-y stage is typically 250 mms in both directions. Any errors in translation introduces an error in the registration of the detector array with respect to the photo co-ordinates of the stationary reference transparency. Hence this error relates not to the measurement of parallax but to the definition of x-y location on the transparency at which the parallax has been measured. The measured parallax in all automated stereo compilation instruments represents an average

over the correlation area which in this case is 500x500 micrometers. Hence errors of the order of 25 micrometers in the definition of the center of the correlation areas will have an insignificant effect on the accuracy of the computed digital terrain model. Translation stages having a precision and accuracy of the order of 25 micrometers over a translation distance of 250 mm are common and represent off the shelf technology. However if the two transparencies were to be mounted independently on two stages, the translation errors would reflect directly on the measurement of parallax, necessitating the need for high precision and expensive translation stage systems.

The errors in the image scanning translation stages can be thought of as slope errors and therefore their contribution to the final data can be considerably reduced by post measurement data smoothing and data processing. Also by overlapping adjacent blocks of data, large translation errors due to system drop out can be detected and the continuity of the measured data assured. The above discussions clearly indicate that the requirement for mechanical scanning of the input transparencies does not pose serious impediments to the application of HOC systems in the field.

#### 4.5 Evaluation of Array Detector Sensitivity and Laser Power Requirements

The basic concept of the HOC system requires that the two superimposed light distributions at the final image plane be coherent with each other. Laser provides a means of obtaining high intensity monochromatic illumination that can be efficiently coupled into the interferometer. The type of laser that needs to be used in the prototype HOC system is a significant factor that has impact on the feasibility and applicability of the system in field applications. The requirement for a large power water cooled Argon Ion laser would significantly reduce the feasibility of the concept of a rugged and compact

HOC system. In this section the factors that determine the laser power requirements are outlined and calculations are presented to show that a small and simple He-Ne laser would meet the illumination requirement.

The detector arrays are integration devices and hence their sensitivity depends on the speed of operation. While large integration times are preferred from the point of view of low laser power, the measurements have to be fast enough to make the instrument insensitive to vibration. As pointed out earlier in Section 4.1 the clock frequency for the detector array must be around 400 KHz in order to make the system insensitive to most of the mechanical and building vibration. The exposure requirements for the detector array can be calculated as follows:

The saturation exposure for the array:	.3 $\mu$ watt sec/cm <sup>2</sup>
Integration time at 400 KHz:	6.25 msec
The saturation power density:	50 $\mu$ watts/cm <sup>2</sup>
TOTAL illuminated area:	6.25 cm <sup>2</sup>
TOTAL power required:	.3 mwatts.

Assume an optical coupling efficiency of 20%.

TOTAL diffracted power:	1.5 mwatts
-------------------------	------------

Assuming 5% diffraction efficiency for the structure information on the transparencies, total laser power required is 30 mwatts. This power can still be further reduced by lowering the clock frequency if necessary. He-Ne lasers capable of providing 30 to 40 mwatts of output are typically 3 to 4 feet in length and they do not require special power or water cooling provisions. Such lasers are now becoming a common OEM item in computer output laser printers and hence they represent reliable and field proven components for the final system.

#### 4.6 Evaluation of the Effect of Input Transparency Format Geometry on the Performance of the HOC System

Conjugate image matching is a basic element of all stereogrammetric operations. Manual methods of stereo compilation rely on stereoscopic perception and acuity of the human operator to achieve conjugate image matching. In automated stereo- compilation instruments the conjugate image coincidence is detected using image correlation. Image correlation involves the examination of the similarity of the image structure being superimposed to ascertain whether they are conjugate images. Slope and perspective distortions, difference in scale between transparencies and other geometrical distortions in the transparencies cause dissimilarity between conjugate images. This results in reduced signal to noise of conjugate image coincidence detection. In some of the electronic correlation systems by shaping the scan process, the problems of dissimilarity can be overcome. It is possible to introduce continuously variable anamorphic and spherical zoom optics in both channels of the HOC interferometer to overcome distortion between conjugate images. In fact in the Gestalt photomapper, the scanning raster is shaped over a 50x50 matrix of correlation errors and such a shaping can be implemented in the HOC system. However from a practical viewpoint such additions to the basic HOC configuration make the over all optomechanical systems too complex and the control problem cumbersome. Inability of HOC type optical system to continually adopt to the changing input format geometries is a compromise that must be made. While it is theoretically possible to design optical systems to provide nonlinear distortion corrections, such systems are not yet practical in the field environment. In this section the ability of the HOC system to utilize unrectified convergent input transparencies for compilation is evaluated.

Convergent photography consists of two oblique photographs taken with two cameras, with one tilted forward along the flight direction

and the other tilted backward. Convergent photography enables a large base to height ratio to be obtained and yet achieve 100 percent end lap. Since the convergent photographs are simply low oblique photographs, they can be analyzed as any tilted photos to determine scale, relief displacement, tilt displacement, ground point coordinates etc. In order to evaluate the feasibility of HOC concept to convergent pairs, the parameter that is of importance is the rate of change of scale across the transparency.

Consider the geometry of the tilted photograph illustrated in Figure (4.1). Tilt is considered here to be the single resultant tilt that is a vector addition of the components usually referred to as tip and tilt. In convergent photography the tilt direct is also the flight direction. While the scale of the photography changes along the direction of tilt, the scale does not change along any line that is perpendicular to the direction of the tilt. However between the transparencies, the scale is approximately equal along only one line that is perpendicular to the direction of tilt and is different everywhere else.

In order to utilize the two dimensional cross correlation of conjugate images to detect their coincidence, it is essential that the conjugate images are similar in scale along both x and y directions. Since the change in scale between conjugate images in the two transparencies is in the opposite directions of the nominal value, the dissimilarity between the conjugate images would drastically reduce the detectability of the point of coincidence. While it is difficult to derive the exact relationship between difference in scale and the broadening effect on the correlation function, based on empirical evidence it can be stated that difference in scale between conjugate images should be less than 10%.

Using the notation and the mathematics outline in Reference (4), the scale of any image on a tilted photograph can be expressed as

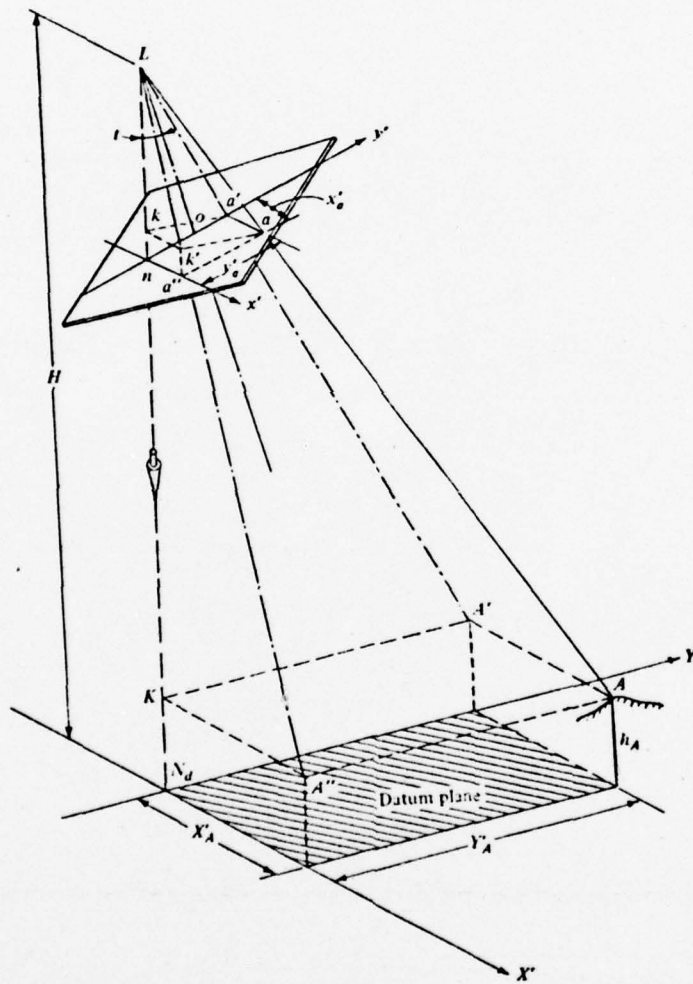
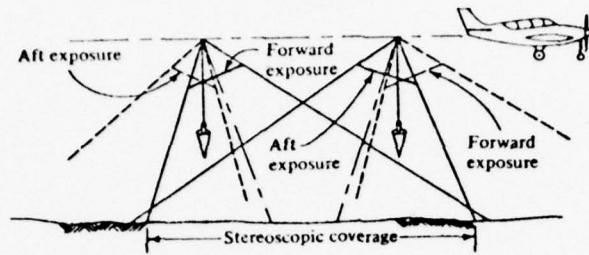


Figure 4.1 Geometry of Convergent Photographs

$$S = \frac{f - y \sin t}{H - h}$$

where  $t$  is the tilt,  $y$  is the distance of the image from the isocenter measured in the direction of the tilt,  $f$  is the focal length,  $H$  is the flying height and  $h$  is the height of object point. Let us consider an example of convergent photography. Ideally,

$$\tan t = \frac{B}{2H}$$

Assuming  $B/H \approx 1$ ,

$$\tan t = .5$$

$$t = 25.5^\circ$$

$$\sin t = .447.$$

At the isocenter

$$S_0 = \frac{f}{H - h}$$

At the extreme point in the format

$$S_1' = \frac{f - y(.447)}{H - h}$$

Change in scale

$$S_0 - S_1' = \frac{.447 y}{H - h}$$

The difference between two conjugate images is given by

$$\Delta S_p = \frac{2 \times (.447) y}{H - h}$$

$$\approx \frac{y}{H-h}$$

Percentage change in scale

$$\frac{\Delta S_p}{S_0} \approx \frac{y}{f}$$

If the tolerance on the scale between conjugate images has to be met, the area on the transparency bounded by the half field angle is approximately  $6^\circ$ .

This is too small an area and the discussion presented above clearly indicates that it is not feasible to directly use the unrectified convergent photography in a HOC system.

The discussions presented above do not apply to the case of panoramic photography. A panoramic photograph is a picture of a strip of terrain taken transverse to the direction of flight. The geometry of the panoramic photograph is shown in Figure (4.2), along with an illustration of the stereoscopic overlap between a pair of vertical panoramic photos. Using the parameters defined in Figure (4.2) it can be shown that (5), the scale  $S_x$  at any point of a vertical panoramic phase is

$$S_x = \frac{f \cos}{H - h}$$

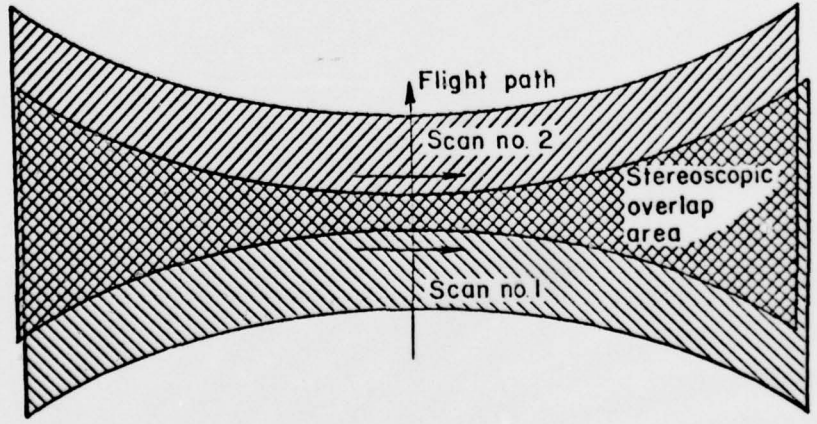
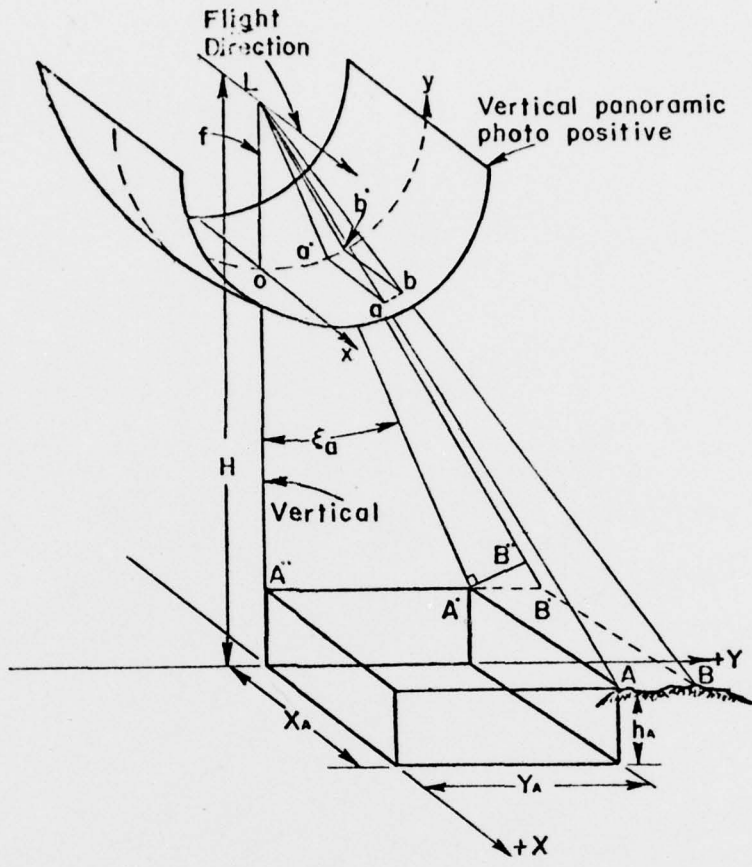


Figure 4.2 Panoramic Photo Geometry

Where  $f$  is the focal length,  $\xi$  is the scan angle,  $H$  is the flying height and  $h$  is the elevation of the object point above datum. Also the scale along the  $y$  direction is given by

$$S_y = S_x \cos \xi \quad (\text{see Reference 5})$$

The scale of the imagery within a photo varies continuously from point to point. Let us consider the scale of the conjugate images in a stereo-pair. As illustrated in Figure (4.2), the conjugate image lies on an  $x$  strip of the conjugate images or very nearly the same scan angle. Hence the scale of the conjugate images in both  $x$  and  $y$  directions have to be nearly the same. It is the difference in scale between conjugate images that is important from the point of view of operation of the HOC. The geometrical distortion of the panoramic stereo pair represents no hindrance to the applicability of the HOC concept. The feasibility of the HOC instrument to accommodate panoramic input transparencies depends only on the complexity of the post detection data processing requirements.

#### 4.7 Summary

In this chapter the feasibility and applicability of the HOC system for field applications has been evaluated by considering the tolerance specifications of the optical, mechanical and electronic subsystems as a function of the performance requirements. The analysis presented show that the HOC system can be configured to be less sensitive to vibration, thermal and mechanical drifts and other instabilities inherent in the field environment.

## 5 PROPOSED PROTOTYPE HOC SYSTEM DESIGN

### 5.1 Introduction

The discussions presented in Chapter 4 clearly indicate that the HOC system is a potential candidate for a van mounted stereo model digitizer. In this chapter a conceptual design of a prototype HOC system is presented. The unique characteristics of such a system are outlined and its advantages over other automated electronic stereo-compilation systems are described. Some of the hardware design details are presented to emphasize the feasibility and availability of the various system components. The prototype HOC system can be subdivided into optical, mechanical, and electronic subsystems. In this chapter each of these subsystems are described independently.

### 5.2 System Description

#### 5.2.1 Optical System

The optical configuration of the proposed prototype HOC system is illustrated in Figure 5.1, and the actual layout is shown in Figure 5.2. Light from a HeNe laser is directed into the two channels of the interferometer with the 50/50 dielectric beam splitter. Electronically operated shutter S, permits selective illumination of one of the transparencies. The modulator M is used to shift the optical path difference between the two channels of the interferometer. The illuminating optics in each channel of the interferometer consist of a beam diverger and a condenser lens. The folding mirrors permit the transparencies  $T_1$  and  $T_2$  as well as the translation stages on which they are mounted to be horizontal. The horizontal mounting of the stages and the transparencies assure mechanical stability and speed of translation. The condenser lens is mounted behind the transparencies as close as possible so that the diameter of the condensing optics need not be much larger than

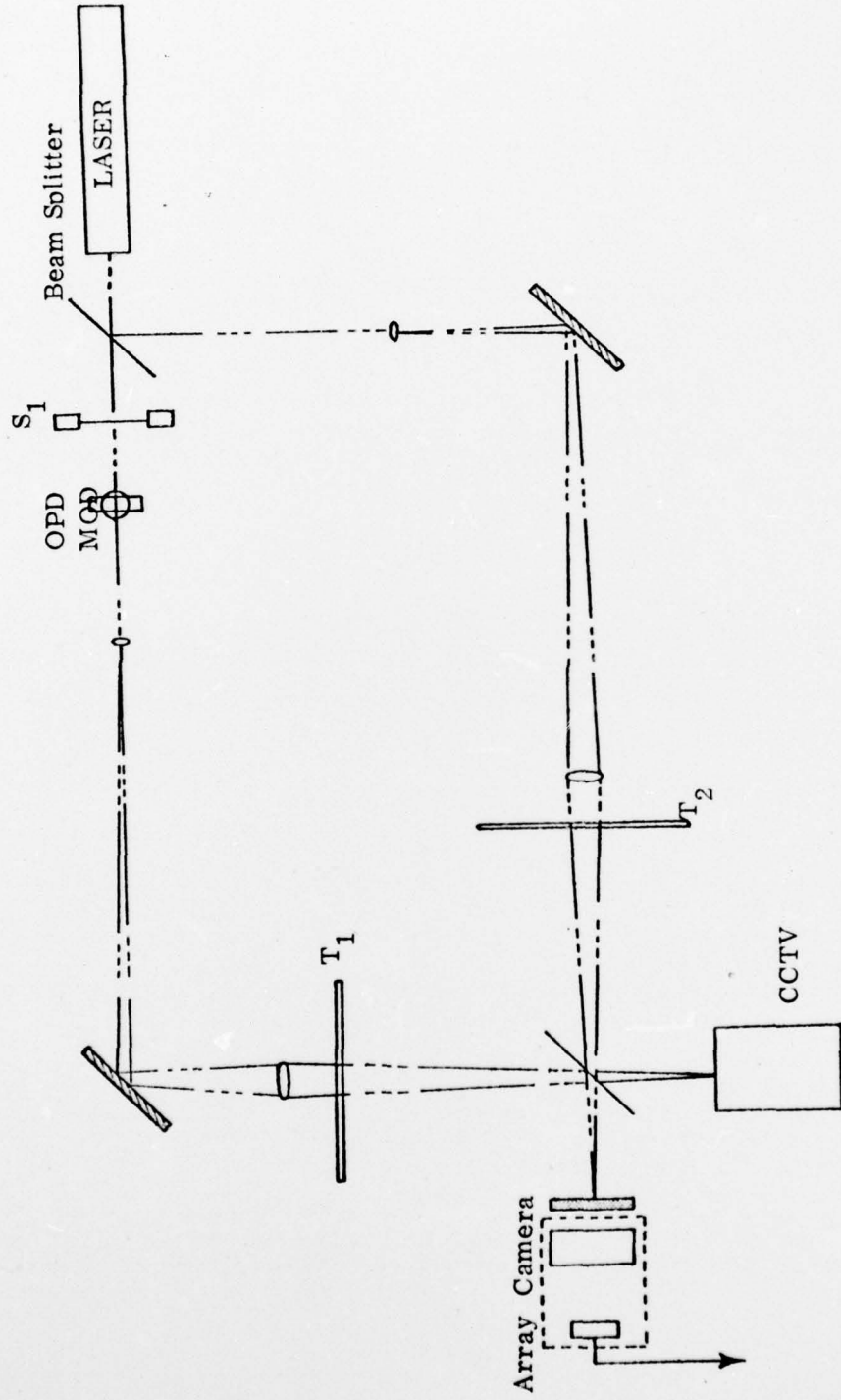


Figure 5. 1 Optical Configuration of HOC Prototype System

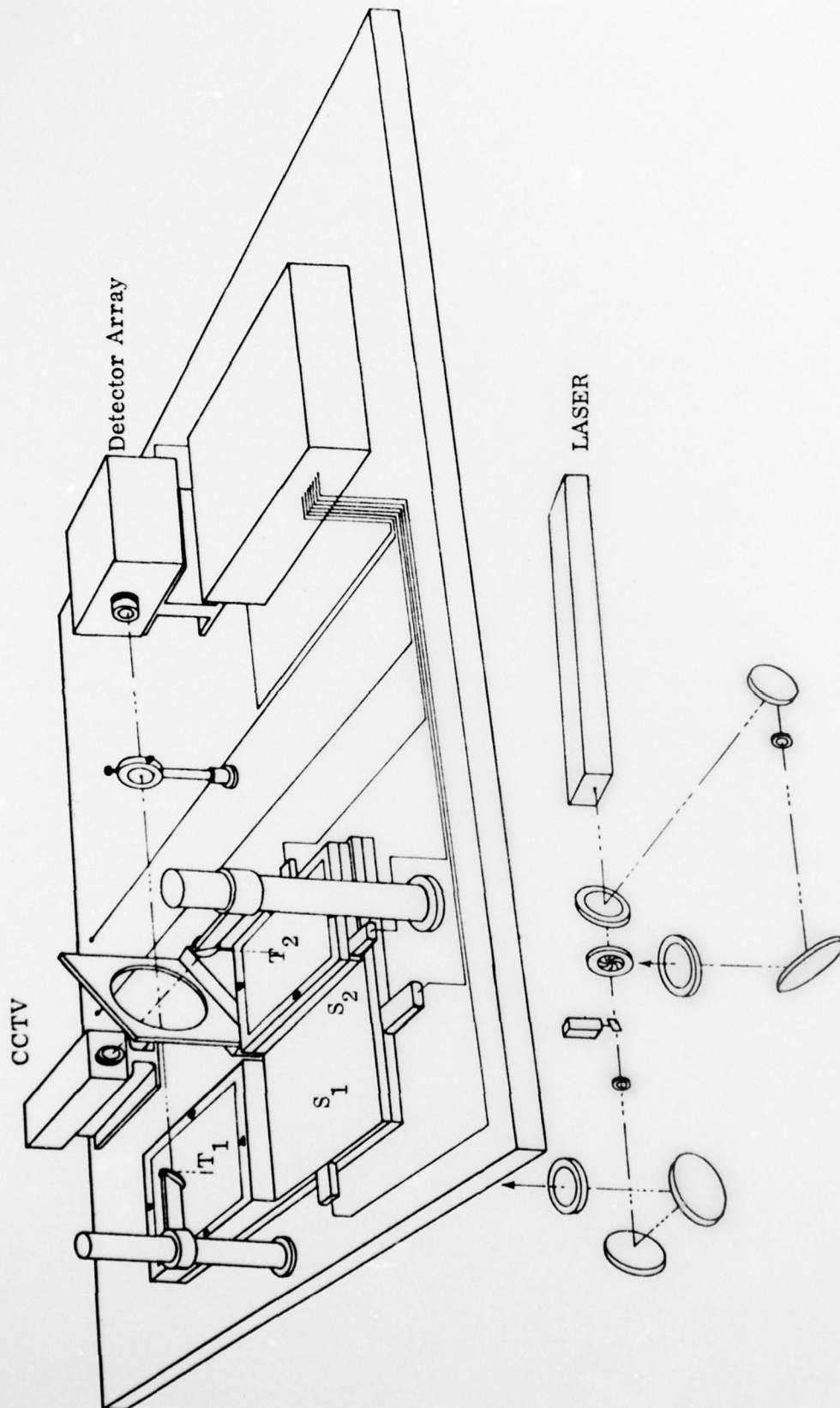


Figure 5.2 Proposed System Configuration for HOC

the area being illuminated. The final imaging lens, which is a part of the detector array camera, produces superimposed images of the transparencies at the common image plane occupied by the detector array. The d-c block is located between the final beam splitter and imaging lens. The final beam splitter has two output beams that are normal to each other. One of the beam paths, as described earlier, is directed to the array camera. The other is directed to a Vidicon camera-closed circuit TV system so as to permit the examination and display of the superimposed images of the transparencies. The display of the common image plane permits the initial manual relative orientation of the transparencies. It is to be emphasized here that the optics used are neither complex nor high precision and most of the components are comparatively small in size. The base plate shown in Figure 5.2 is expected to be approximately 5 feet by 3 feet in size and that provides an idea of the overall size of the instrument.

### 5.2.2 Mechanical System

The mechanical part of the system consists of the translation stages, the transparency holder, the mechanical mounts for the optics and the overall support for the instrument. For the sake of brevity only the design aspects of the translation stages and the transparency holders are discussed in detail in this section. The basic design characteristics of the mechanical mounts for the optical components and the overall instrument support must be mechanically rigid. By proper mechanical design many of the component mounts can be made non-kinematic, thereby alleviating some of the alignment drift problems.

The conceptual design of the translation stages and their requirements have already been described in Chapter 3. The transparency  $T_1$  is directly mounted on the large xy Stage  $S_1$ . Transparency  $T_1$

is the reference transparency having a direct orientation relationship to the diode array. Hence the measurement accuracy of the stage  $S_1$  is important from the point of view of defining the correlation areas on the plane of the reference transparency  $T_1$ . The transparency  $T_2$  forming the stereo-pair is mounted on top of an  $xy$  stage  $S_2$  which in turn is mounted on the large stage  $S_1$ . The stage  $S_2$  permits relative translation between transparencies  $T_1$  and  $T_2$  which is needed for parallax measurement. For most anticipated applications of this instrument the maximum relative translation between the translation transparencies is expected to be less than an inch. Hence, while the stage  $S_2$  has to be large so as to hold the transparency  $T_2$ , the maximum translation in both  $xy$  direction need not be greater than an inch. The accuracy and precision of the stage  $S_2$  is critical since, the measurements made with  $S_2$  directly represent  $x$  and  $y$  parallax values. The stages can be driven with stepping motors directly by the control computer and encoders can be used to provide positional information. The use of encoders instead of the stepping motors to obtain positional information on the transparencies avoids the requirement for initialization and continuous tracking. The transparencies can be mounted outside the instrument on plate holders such that the reference marks on the holders precisely coincide with the regular or marked fiducials on the transparencies. The holders can be designed and fabricated such that they can be located precisely on the stages. Thus the initialization and relative orientation of the transparencies on the holders can be achieved easily outside of the instrument. Once the coordinate system defined by fiducials on the transparency is aligned and located with respect to the coordinate system of the stages, the initialization of the instrument for compilation can be achieved directly by the control computer using the aerotriangulation data. Hence the operator interaction with the instrument during the start up phase involves the relative alignment of the fiducials or other marked points on the transparency with the corresponding points on the plate holder.

### 5.2.3 The Electronic System

The electronic system consists of the detector array, the interface electronics, the shutter control, the drive and monitoring electronics associated with the translation stages, the phase modulator, the closed circuit T. V. Monitor and the control computer. The specifications and requirements of these various components are standard and represent "off-the-shelf" technology. Detailed discussion of the various electronic components of the system are beyond the scope of this report. In this section, the data processing hardware requirements and the speed of operation of the system are discussed, so as to demonstrate the viability of HOC as a field instrument.

For the purpose of computing the correlation coefficient for any given orientation between transparencies, four sets of measurements of the detector array are required. Including the memory requirement for storing the dark current values for each element of the array, that represents a requirement for 12.5K of eight bit memory (bytes). Once the correlation coefficient is computed and processed the results stored represent three sets of 2500 data values representing the maximum correlation coefficient, the  $p_x$  step at which the maximum occurred and the  $p_y$  step at which the minimum occurred. This part requires 7.5K bytes. Hence for computing the x and y parallax values for a given 50x50 correlation area in the stereo model, the storage requirements can be easily met by the capabilities of a minicomputer. Since the data corresponding to the entire stereomodel represents 300,000 values, the x and y parallax values must be periodically transmitted onto magnetic tape during translation between one set of correlation areas to another within the stereomodel.

The speed of operation of the potential instrument can be illustrated by considering a hardened and field compatible minicomputer

such as PDP 11/34M as an example for the control computer. As stated earlier four sets of intensity measurements with the detector array are needed for the computation of the correlation coefficient. Consider the array operating at 400 KHz clock rate. This means that the sample and hold and the A/D converter must be fast enough to obtain 8 bit A/D conversion within 2.5 microseconds. The time budget for the overall measurement is computed as follows:

Time taken to read a frame:	6.25 milliseconds
Assuming four frame averaging, the time for one measurement is:	25 milliseconds
Time delay between subsequent measurements:	6.25 milliseconds
Time for four sets of measurements:	118.75 milliseconds

Let us now consider the time required to compute the correlation coefficient. The time required for computing the correlation coefficient at each point (for PDP 11/34M) is 100 microseconds.

Computation time for the array:	250 milliseconds
Total time required for each step:	.350 milliseconds
Assuming 100 $p_x$ steps and 5 $p_y$ step, total steps:	500
Total time for compiling 50x50 array of points on the model	approximately 3 min.

Nominally 50x50 array of correlation areas cover a 25 mm square on the model. There are typically 50 such areas. The time required for translation between different areas on the model are insignificant compared to the compilation time for each step. Hence the total anticipated time for computing the parallax values for each model (150x200 mm) is approximately 150 minutes.

It is to be emphasized here that the parallax values measured refer to the photo-coordinate system of the stationary transparency and is identical to the data that can be obtained from a stereo comparator. The computation of the ground data from the HOC data is straight forward and has been outlined in Reference (3). It is proposed that this data processing is done outside the HOC instrument, probably using the same control computer after the measurement process.

### 5.3 Data Processing Requirements

As stated earlier the output from the basic HOC system represents the  $x$  and  $y$  parallax values of an array of elemental correlation areas defined on one of the transparencies. This data can easily be reduced to provide the coordinates of the corresponding areas in the second transparency. If  $M_1, M_2$  are the exterior orientation matrices (object to photo) and  $f$  the focal length, then the coordinates on two equivalent truly vertical photographs (assuming positive geometry) are:

$$\begin{bmatrix} u \\ v \\ w \end{bmatrix} = M_1^t \begin{bmatrix} x \\ y \\ -f \end{bmatrix} \quad \text{and} \quad \begin{bmatrix} u' \\ v' \\ w' \end{bmatrix} = M_2^t \begin{bmatrix} x' \\ y' \\ -f \end{bmatrix} \quad (5.1)$$

when  $(x, y)$  is the coordinates in photo 1 and  $(x', y')$  is the coordinate in photo 2.

Let  $X_{c_1}, Y_{c_1}, Z_{c_1}$  and  $X_{c_2}, Y_{c_2}, Z_{c_2}$  be the coordinates (in the object space) of the two camera stations, and  $X, Y, Z$  the object coordinates of any point, then

$$\begin{bmatrix} X-X_{c_1} \\ Y-Y_{c_1} \\ Z-Z_{c_1} \end{bmatrix} = t_1 \begin{bmatrix} u \\ v \\ w \end{bmatrix} \quad \text{and} \quad \begin{bmatrix} X-X_{c_2} \\ Y-Y_{c_2} \\ Z-Z_{c_2} \end{bmatrix} = t_2 \begin{bmatrix} u' \\ v' \\ w' \end{bmatrix} \quad (5.2)$$

where  $t_1$  and  $t_2$  are scale factors, which when eliminated lead to

$$\frac{(X-X_{c_1})}{(Z-Z_{c_1})} = \frac{u}{w} \quad \text{and} \quad \frac{(X-X_{c_2})}{(Z-Z_{c_2})} = \frac{u'}{w'}$$

Then,

$$X = X_{c_1} + \frac{u}{w} (Z-Z_{c_1}) = X_{c_2} + \frac{u'}{w'} (Z-Z_{c_2}) \quad (5.3)$$

$$Z \left( \frac{u}{w} - \frac{u'}{w'} \right) = \frac{u}{w} Z_{c_1} - \frac{u'}{w'} Z_{c_2} + X_{c_2} - X_{c_1}$$

$$Z \frac{uw' - u'w}{ww'} = \frac{uw' Z_{c_1} - u'w Z_{c_2} + ww' B_X}{ww'}$$

$$\text{where } B_X = X_{c_2} - X_{c_1}$$

or

$$Z = \frac{uw' Z_{c_1} - u'w Z_{c_2} + ww' B_X}{uw' - u'w} \quad (5.4)$$

and

$$Y = Y_{c_1} + \frac{v}{w} (Z-Z_{c_1}) = Y_{c_2} + \frac{v'}{w'} (Z-Z_{c_2}) \quad (5.5)$$

Equations 5.3, 5.4 and 5.5 may be used to compute the ground coordinates corresponding to each elemental correlation area on the transparencies.

Since the ground coordinates measured represent regularly sampled data in the plane of the transparency, the transformed points in the object space represent irregularly sampled data points. It is necessary for all subsequent utilization that this irregularly gridded data be converted to regularly gridded data points. Also the raw HOC data contains points at which no correlation has been performed due to lack of image structure. It is also possible that some data points measured might be inconsistent with the nature of the terrain being compiled. Hence the processing of HOC data is necessary not only from the point of view of transformation but is also required to obtain data smoothing. Considerable work has already been accomplished with regard to the problem of surface modeling (6). In these techniques the surface is represented as a family of locally valid mathematical functions which join together continuously. Either the elaborate discussion of this procedure or its hardware requirement are beyond the scope of this report. However it is to be noted that this problem has been successfully handled as it applies to automated cartography and hence is readily available for implementation. This procedure permits one to smooth small peaks and depressions caused either by discreteness of data or by localized errors.

#### 5.4 Unique Characterization of the Proposed HOC System

The unique characteristics of the proposed HOC system as compared to other automated stereo compilers include:

- (a) In the HOC system no operator interaction after the initial set up is required. Unlike the electronic correlation system, the HOC is not a tracking correlator. The ability

to detect conjugate image coincidence in any given elemental area does not in any way depend on the correlat-ability of the neighboring elemental areas. Hence the problem of "getting lost" is irrelevant to the HOC system. This minimizes the operator intervention.

(b) As an area correlation system the HOC is potentially capable of greater accuracy and reduced uncertainty in parallax measurement, however this remains to be proven. The demonstrated accuracy in parallax measurement under conditions of ideal imagery is about 5 micrometers.

(c) Because of the simplicity of construction and operation the HOC system is potentially less expensive and easier to maintain than more complex electronic correlators.

(d) It is feasible to use microprocessors instead of mini-computers to control the HOC operation and data management, at the expense of reduced operational speed. Hence the entire system can be made as compact, rugged and portable as a mechanical plotter.

(e) Finally the HOC system is based on a detection concept that is analytically superior to one-dimensional electronic correlation system. The components and the technology proposed are being continuously improved in terms of cost and performance. Hence the HOC system development will be consistent with the trend in technology.

## 6 CONCLUSIONS AND RECOMMENDATIONS

### 6.1 Introduction

This report summarizes results of the design and feasibility study of HOC as a van mounted stereomodel digitizer. In this report the system model of the HOC used for evaluation has been described and the applicability and the feasibility of HOC system under field conditions have been evaluated. Based on the results of the study a follow-on prototype design for the field compatible HOC system has been proposed. In this chapter the conclusions of this investigation are listed and the specific recommendations are outlined.

The results of this investigation support the following general conclusions:

- (a) It seems feasible that a HOC system can be configured to be small, compact and rigid to be used as a van mounted stereomodel digitizer.
- (b) An evaluation of the optical and mechanical subsystems indicate that a potential HOC system can be made less sensitive to mechanical and thermal instabilities inherent in any field applications.
- (c) The control and processing requirements of the HOC are simple enough to be handled by a minicomputer that is compatible for van mounted operation.
- (d) The proposed system approach to HOC system configuration is such to limit its ability to handle imagery in which the scales of conjugate images are highly dissimilar. While this limitation does not exclude panoramic input, the HOC system as proposed will not be able to handle highly convergent inputs. However

the convergent inputs can be rectified in an off line mode before compilation by the HOC system. This proposed inflexibility of the HOC represents the price paid for achieving a more field compatible and simple instrument.

(e) The control and data processing requirements of the proposed system are neither large nor complex. The speed of operation of the instrument in light of the simplicity of the data processing hardware used represents a major advantage.

(f) Finally, the overall evaluation of this study indicates that the HOC is not only feasible but has many unique advantages in its application as a van mounted stereomodel digitizer.

## 6.2 Recommendations

The specific recommendations of this study are:

(a) A follow-on prototype HOC system should be designed fabricated. An exhaustive "field" evaluation of such a system would clearly demonstrate the conclusions of this report.

(b) Evaluate the applicability of the off-line orthoprinter as a general purpose input transparency rectifier for the HOC system. The preprocessing of the input transparency has many advantages interms of improved signal to noise ratio in coincidence detection, uniformity of accuracy and simplicity of the over system requirements.

This study has revealed that a HOC system has great potential as a van mounted stereomodel digitizer. The construction and evaluation of the follow-on prototype HOC system will demonstrate its advantages over other competitive systems particularly in a field environment.

## 7 REFERENCES

- (1) Balasubramanian, N. and R. D. Leighty, Heterodyne Optical Correlation Photogrammetric Engineering, Vol. 42, No. 12, Page 1529, 1976
- (2) Balasubramanian, N., "Esperimental Heterodyne Optical Correlator (HOC)," U. S. Army Engineer Topographic Laboratories Final Report No. ETL-0071, October 1976.
- (3) Mikhail, E. M., Photogrammetric Aspects of the Heterodyne Optical Correlator, Final Technical Report - Contract DAAG29-7b-D-0100, Research Institute, U. S. A. E. T. L., July 1976
- (4) Thompson, M. M. (Ed), 1966, Manual of Photogrammetry, American Society of Photogrammetry, Falls Church, Va., Chapter 15
- (5) Wolf, P. R., 1974, Elements of Photogrammetry McGraw Hill, Inc.
- (6) Jancaitis, J. R. and Junkins, J. L., Modeling of Irregular Surfaces, Photogrammetric Engineering, Vol. 39, Page 413, 1973